Journal of Applied Polymer Science

# Morphologically dependent alternating-current and direct-current breakdown strength in silica–polypropylene nanocomposites

**Timothy Krentz,[1] Mohammad M. Khani,[2] Michael Bell,[2] Brian C. Benicewicz,[2] J. Keith Nelson,[1] Su Zhao,[3] Henrik Hillborg,[3] Linda S. Schadler[1]**

[1]Department of Materials Science and Engineering, Rensselaer Polytechnic Institute, 110 8th Street MRC 140, Troy, New York 12180

[2]Department of Chemistry and Biochemistry, University of South Carolina, 541 Main Street, Horizon I Room 232, Columbia, South Carolina 29208

[3]Power Devices, Corporate Research, ABB AB, Forskargränd 7, Västerås 721 78, Sweden

Correspondence to: T. Krentz (E-mail: krentz.tim@gmail.com)

**ABSTRACT:** In this article, we report the synthesis of a new bimodal surface ligand morphology on silica nanoparticles. Combining grafting-to and grafting-from approaches, in this study, we demonstrated the efficacy of anthracene surface modification for improving the dielectric breakdown strength (DBS) under alternating-current and direct-current conditions and that of a matrix-compatible polymer brush for controlling the nanofiller (NF) dispersion. Ligand-modified spherical colloidal $SiO_2$ nanoparticles (~14 nm in diameter) were mixed into polypropylene, and the resulting dispersion was improved over the unmodified particles, as shown with transmission electron microscopy. The results suggest that the electronic structure of the anthracene-modified particle surface was critical to the improvement in DBS. In addition, the DBS of the composite was shown to depend on the dispersion state of the filler and the mode of stress; this indicated that the individually dispersed nanoparticles were not necessarily the optimal morphology for all stress conditions. Additionally, the precise nature of the matrix-compatible brush was less important than the NF dispersion it produced. The bimodal grafted architectural design has provided a promising solution for the control of the dispersion and surface properties, especially for high-molecular-weight polymer matrices. © 2016 Wiley Periodicals, Inc. J. Appl. Polym. Sci. **2017**, *134*, 44347.

**KEYWORDS:** composites; dielectric materials; nanotechnology; polypropylene

Received 23 May 2016; accepted 5 August 2016
**DOI: 10.1002/app.44347**

## INTRODUCTION

High-voltage capacitors are an enabling technology for high-voltage power transmission.[1] Inorganic nanofillers (NFs) have become an area of focus for use in insulating polymer composites because of the useful properties they exhibit.[2–6] The dispersion of NFs is difficult to control, especially when one scales up from laboratory to industrial processing.[7,8] Agglomeration is typically driven by the hydrophilic nature of the NF or the use of surface modifiers to improve properties[9] that are enthalpically incompatible with the matrix. In this study, a surface modification method was used to independently control the dispersion and dielectric properties through the use of two populations of surface ligands: one population was small molecules chosen to enhance the high-voltage performance, and one population was a longer matrix-compatible brush to control dispersion.

Although short-molecule surface modification can reduce the filler–matrix enthalpic incompatibility and lead to a relatively good dispersion,[10] the filler interaction with the matrix is limited to van der Waals forces, and the choice of ligand is limited to those enthalpically compatible with the matrix. To add functionality to the filler surface with short molecules, a longer polymer brush is needed to shield the enthalpic effects and can also control entropic penalties within high-molecular-weight polymer matrices.[11–13] These bimodal brushes have been shown to be effective for controlling dispersion and adding functionality.[14–16] Models based on these principles have been effective for predicting nanoparticle dispersion states in homopolymer melts.[14,15,17]

Electron avalanches were assumed here to be the dominant mechanism for the dielectric breakdown of polypropylene, as in other olefins.[18] Avalanches occur when, under high field, electrons injected from the electrode gain sufficient energy for impact ionization; this leads to charge multiplication.[19,20] Dielectric breakdown strength (DBS) can be improved, therefore, through the introduction of extrinsic trap states, such as

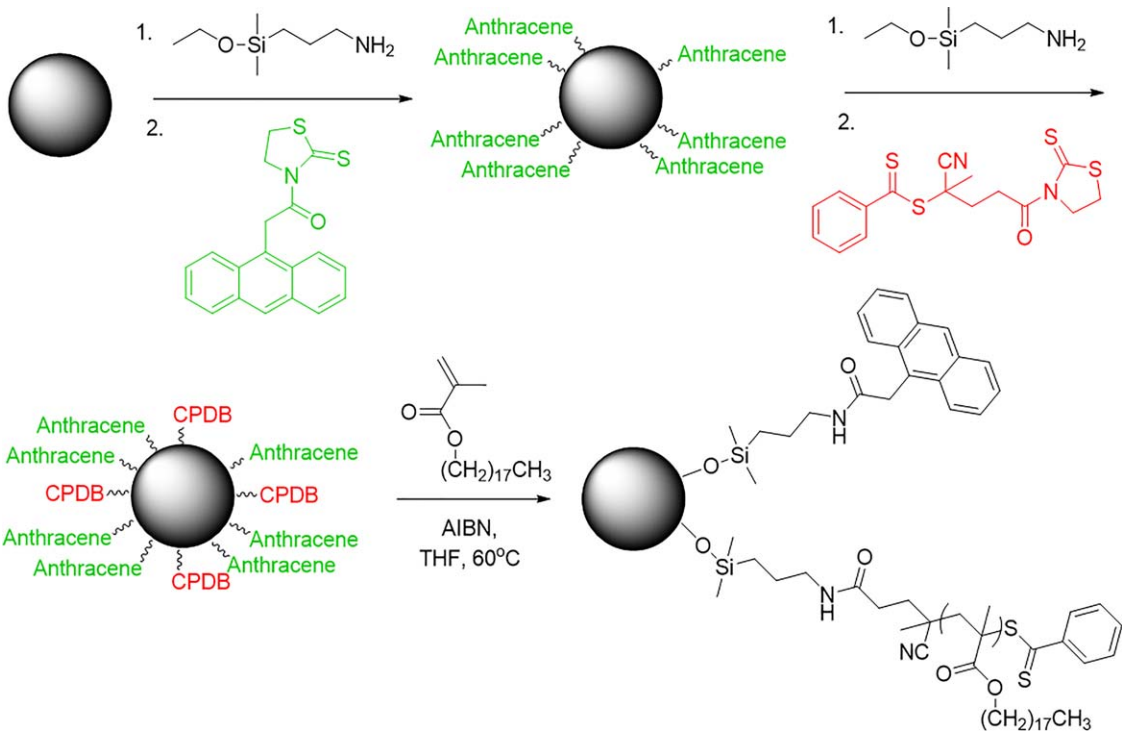


**Figure 1.** Schematic of the bimodal surface modification of the silica nanoparticles. [Color figure can be viewed at wileyonlinelibrary.com]

those available on the NF, which slows charge mobility and buildup.[21–23] Previous work from our group demonstrated that when anthracene was grafted to NFs, the DBS of the epoxy improved when the NFs were well dispersed.[16] Although some studies have indicated that it also may improve DBS as a free additive in some systems,[18,24] this study indicated that free anthracene molecules reduced DBS in polypropylene, and this was likely related to increased conductivity.[25] The DBS improvements seen in systems with anthracene have been attributed to trap states for electrons associated with the anthracene molecule, be they at an NF surface (in this study) or in phase-separated regions. These trap states have been hypothesized to allow energetic electrons to fall into lower energy states and reduce impact ionization events; this would reduce the ability of avalanches to reach a critical size. Thus, in addition to the trapping functionality introduced by anthracene, dispersion control is critical, as an avalanche must encounter a filler particle before it reaches a critical size. Seitz[26] suggested that avalanches can reach a critical size around 200 nm, and this provides a threshold for an interparticle spacing that should be attained for the composite to experience improvements in DBS. Finally, bimodally modified oxide fillers have also shown promise when they were used to improve the permittivity and energy storage in polymer matrix composites.[27]

In this study, anthracene surface groups were grafted onto the nanoparticle surface for its electronic properties, and a methacrylate backbone bottle-brush polymer with stearyl side chains [poly(stearyl methacrylate) (PSMA)] was chosen for its ease of synthesis and the compatibility that olefinic side chains created between the brush and the matrix. The dielectric breakdown performance of the composites with a range of dispersions was then investigated under alternating-current (ac) and direct-current (dc) conditions, and measurements of the permittivity were taken. Samples were prepared for ac voltage endurance testing with neat polypropylene from the best performing NC loaded with PSMA and anthracene-surface-modified silica nanoparticles.

## EXPERIMENTAL

Nissan spherical colloidal $SiO_2$ nanoparticles (~14 nm) with a surfactant layer were dispersed in methyl ethyl ketone (MEK–ST; ~30 wt %) and were used as received. The $SiO_2$ nanoparticles with bimodal architecture were prepared by a combination of grafting-to and grafting-from syntheses. Figure 1 shows a schematic of the synthesis of the bimodally modified silica nanoparticles. The attachment of anthracene and chain-transfer agent to silica was conducted as described previously.[16] PSMA was used as the long matrix-compatible brush and was prepared via surface-initiated reversible addition–fragmentation chain-transfer polymerization. After the attachment of anthracene and the chain-transfer agent, the particles were dissolved in tetrahydrofuran (THF) and were subsequently surface-polymerized with a stearyl methacrylate monomer with 2,2′-azobisisobutyronitrile (AIBN) as the initiator. The final product was precipitated into isopropyl alcohol and redispersed in THF. An aliquot of particles was set aside, and the polymer chains were cleaved with hydrofluoric acid for further characterization. The number-average molecular weight and dispersity of the grafted chains were analyzed with a Polymer Laboratories PL-GPC 120

**Table I.** Surface Modification and Composite Processing

| Sample[a] | PSMA brush graft density (chains/nm$^2$)/ Number-average molecular weight (kg/mol) | Small ligands[b] |
|---|---|---|
| As received | Not applicable | Not applicable |
| PSMA1 | 0.13/86 | Not applicable |
| PSMA2 | 0.14/81 | Not applicable |
| Anth1 | 0.13/75 | Anthracene |
| Anth2 | 0.06/80 | Anthracene |
| Anth3 | 0.13/10 | Anthracene |

[a] All samples were prepared by solvent premixing followed by melt compounding except for PSMA2, which was prepared by dry preblending and melt compounding.
[b] $\sigma = 0.3$ molecules/nm$^2$.

gel permeation chromatograph calibrated with poly(methyl methacrylate) standards.

Three batches of bimodally modified silica nanoparticles were created, as shown in Table I. Nanoparticles with only PSMA on the surface were prepared as reference samples. Particles in the THF solution were refluxed with toluene and polypropylene powder (Borclean HB311BF from Borealis AG) for 30 min to allow for the dissolution of the polypropylene. Solvent-based premixing has been reported in the literature to improve dispersion in polymer-based nanocomposites.[28] Solvent was removed in a vacuum oven at 120 °C for 72 hours, and the resulting composite was used as a masterbatch for later processing. TGA indicated small amounts of solvent remaining, but because each control was processed identically, the effects of any minute residual solvent could be discounted in the results discussed later.

The masterbatch was diluted to a 2 wt % loading of silica via melt mixing in a twin-screw Thermo-Haake melt compounder. The melt was mixed at 185 °C and 60 rpm for 10 min. The as-received nanoparticles were mixed in the previous manner as a control. The neat polypropylene control was melt-blended to create pellets from the as-received polymer powder in the same way. Ungrafted PSMA chains were also added to polypropylene for a control with the same procedure. The PSMA2 control, containing silica nanoparticles with a PSMA brush, was prepared without the solvent premixing step to investigate the impact of processing. For this sample, the particles were dried and then combined with neat polypropylene in the melt-mixing step.

Samples for transmission electron microscopy (TEM) imaging were ultramicrotomed to a thickness of 50 nm before they were loaded onto a copper grid for imaging. Differential scanning calorimetry (DSC) and small-angle X-ray scattering (SAXS) were used to characterize the morphology of the formulated composites with well-dispersed fillers according to a common procedure reported in the literature.[29] DSC was conducted at a 10 °C/min scan rate on a TA Instruments Q100. Films for ac breakdown testing were pressed at 185 °C to an approximately 100-μm thickness, and films for dc testing were pressed to an approximately 50-μm thickness. All films were cooled quickly after pressing. These films were tested at a ramp rate of 500 V/s with a 5 mm ball-plane electrode geometry under silicone oil to prevent flashover. Thicker films of approximately 400 μm were prepared in the same manner for dielectric spectroscopy. Samples for voltage endurance were prepared from the neat polypropylene and from the Anth1 and Anth2 systems with a needle-plane geometry. Needles with a nominal tip radius of curvature of 6 μm were imbedded with a 2-mm tip-to-plane separation to create a highly divergent field. The field at the tip was calculated as follows[30]:

$$\text{Field at the tip} = 2V/[r\ln(4d/r)]$$

where $V$ is the applied voltage, $r$ is the tip radius of the curvature, and $d$ is the tip-to-plane spacing.

## RESULTS

### Morphological and Dispersion Effects on DBS

DSC and SAXS in combination revealed significant changes to the semicrystalline morphology of the polypropylene matrix. The best dispersed samples were chosen as examples because we anticipated that the effects of the filler were the most pronounced when it was well dispersed. Lamellar size was calculated from the periodicity measured from the SAXS data according to the procedure described by Bond.[29]

TEM images of the PSMA-modified silica-filled composites are grouped in Figure 2 in order of the qualitatively improved dispersion. Micrographs of PSMA2 displayed elongated agglomerates of silica oriented approximately parallel to the film surface and to each other. Orthogonal agglomerates and transverse cross sections were not found. The strings in the micrographs were hypothesized to be projections of flattened platelike agglomerates with consideration of the biaxial stress state in the hot-pressing procedure. Most likely, the stress applied during molding caused the agglomerates to elongate in directions normal to the applied stress; this yielded a platelike morphology in a parallel stacked arrangement. In the as-received sample, the image displayed clustered agglomerates. Although the sample was still aligned, the aspect ratio was reduced compared to PSMA2. PSMA1 displayed relatively well-dispersed NFs with a greater degree of smaller, isolated agglomerates and some individual nanoparticles. The improved dispersion was due to the higher density of long PSMA chains, which provided enhanced enthalpic screening. Accompanying the TEM images were the breakdown strength data. The improvement of the dispersion improved DBS, and when a "good enough" dispersion was established, the DBS was similar to the neat polymer. Figure 3 displays the micrographs and corresponding ac DBS data from the composites with PSMA and anthracene-surface-modified NFs. The systems with anthracene displayed qualitatively similar dispersion states to those without anthracene. The addition of anthracene amplified the changes to DBS. Well-dispersed NFs with anthracene outperformed the neat polymer, and the system with elongated agglomerates performed more poorly than the similarly dispersed composite without anthracene.

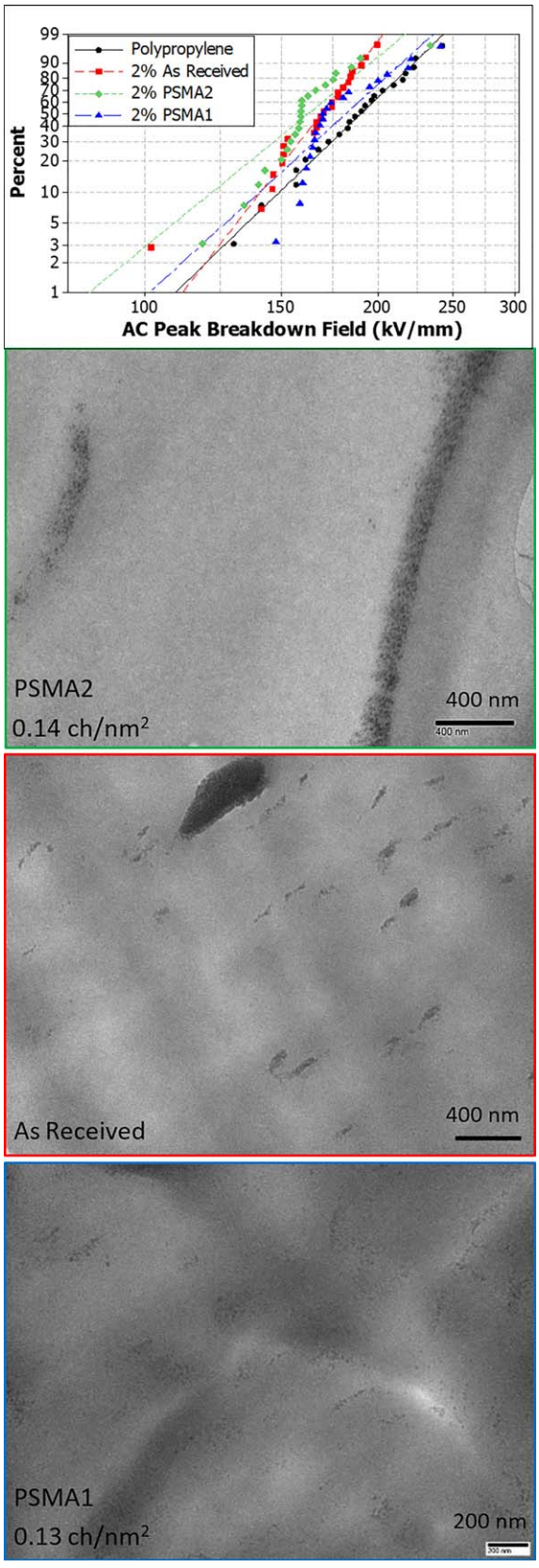


Figure 2. AC breakdown results from the polypropylene control and composites without anthracene surface modification. [Color figure can be viewed at wileyonlinelibrary.com]

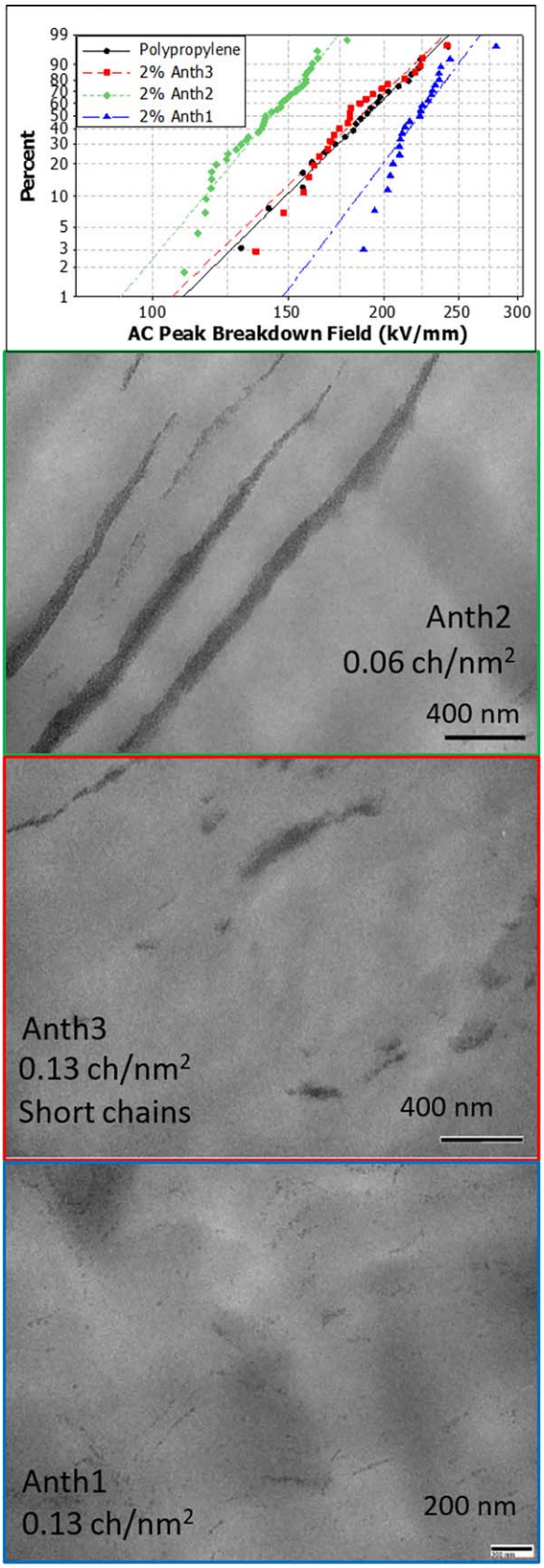


Figure 3. AC breakdown results from the polypropylene control and composites with anthracene surface modification. [Color figure can be viewed at wileyonlinelibrary.com]

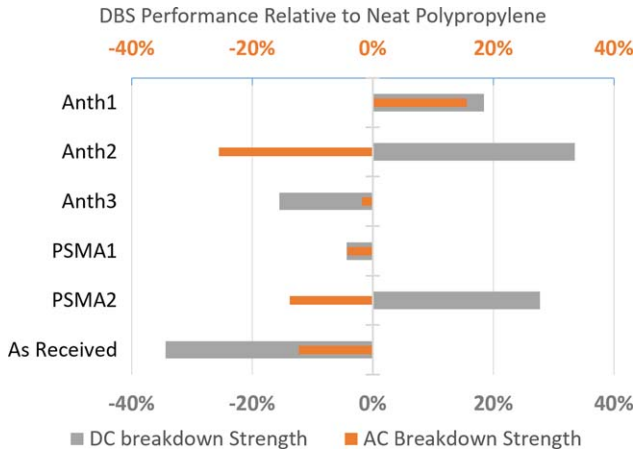


**Figure 4.** Collected 63% characteristic breakdown strength values under AC and DC conditions. [Color figure can be viewed at wileyonlinelibrary.com]

Figure 4 shows the 63% failure probability DBS results from the aforementioned composite systems under dc and ac conditions. Under dc stress, phenomena similar to those under ac were observed in the clustered and dispersed systems. The improved dispersion reduced the decrease in the breakdown strength associated with NFs, and surface modification with anthracene enhanced this effect. The well-dispersed system with anthracene outperformed the neat polypropylene. The effect of the elongated agglomerates observed in PSMA2 and Anth2 was reversed under dc conditions. This led to a significant increase in DBS, whereas under ac stress, the elongated agglomerates led to the highest decrease in DBS. These results and percentage changes in the 63% Weibull scale parameter are collected in Table III (shown later).

### Permittivity

The relative permittivity of the composites compared to the neat polymer baseline is displayed in Figure 5. The composites comprised of silica nanoparticles grafted with PSMA

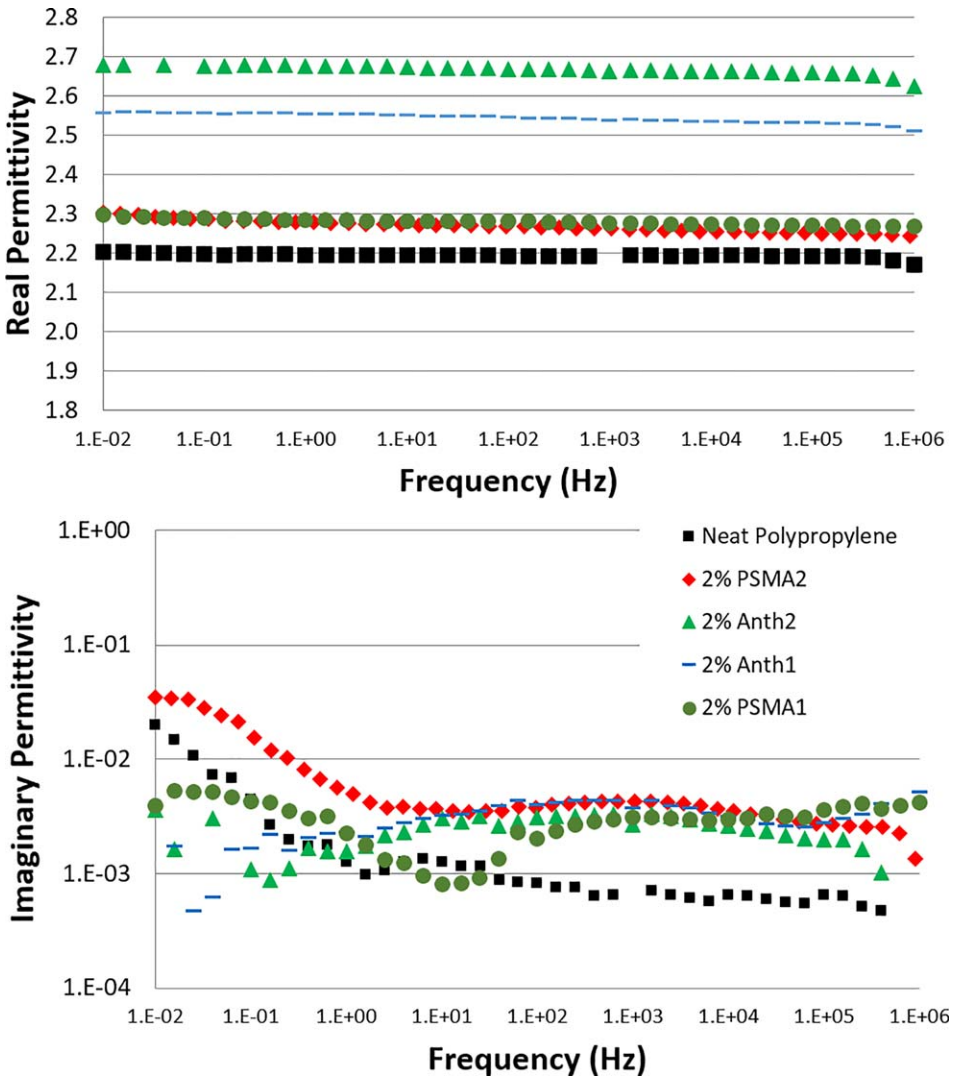


**Figure 5.** Real and imaginary permittivity values from the sample composites compared with neat polypropylene. [Color figure can be viewed at wileyonlinelibrary.com]

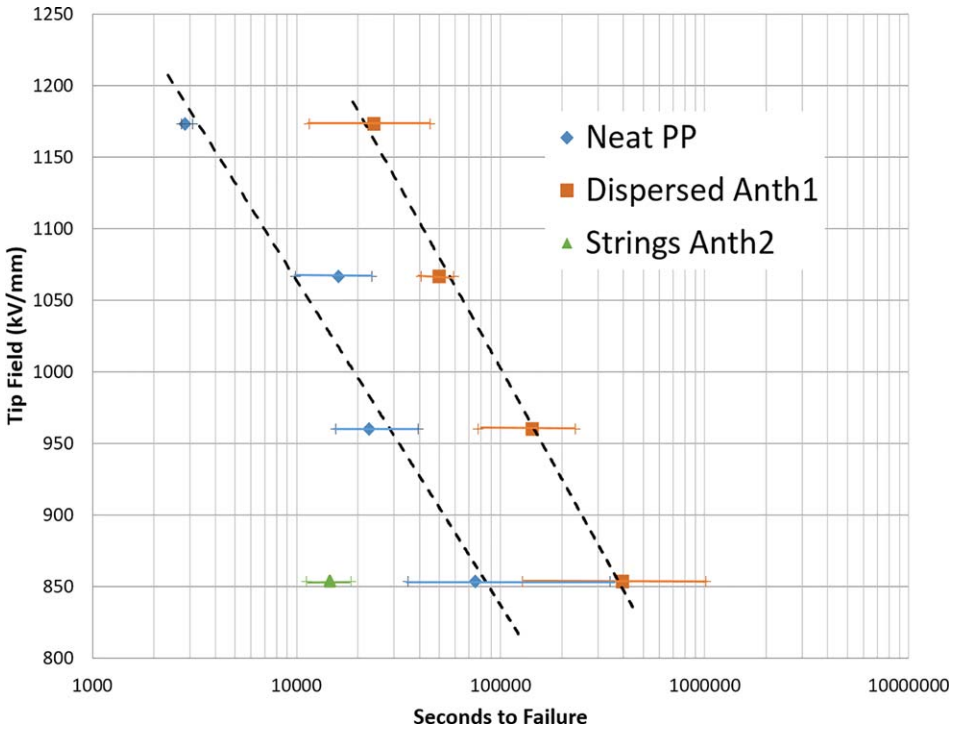


**Figure 6.** Voltage endurance data from the polypropylene (PP) composites under an ac 60-Hz applied voltage. The 95% confidence intervals are shown with tick marks. [Color figure can be viewed at wileyonlinelibrary.com]

demonstrated a peak in the imaginary part of the permittivity, regardless of dispersion. Additionally, while poorly dispersed silica particles increased low-frequency losses, the same morphologies with anthracene showed a reduction in the imaginary permittivity below 1 Hz compared to the systems without anthracene. The improvement in the dispersion also reduced losses at low frequency compared to the elongated agglomerates. The addition of silica particles slightly increased the real part of the permittivity. The anthracene-containing systems displayed an increase in the real permittivity across the entire tested range when compared to their comparably dispersed control composites with brushes comprised only of PGMA. Finally, the elongated agglomerates displayed higher real permittivities than similarly modified dispersed systems.

### Voltage Endurance

To investigate the performance of these composites under time-to-failure conditions, ac test conditions were chosen. Thus, the composite system with the best DBS performance under ac conditions was tested, along with the elongated agglomerate system with anthracene. These are compared in Figure 6 to a neat polypropylene control, whereas the values were in agreement with the literature.[31]

## DISCUSSION

### Morphology and Dispersion

The neat polypropylene, PSMA1, and Anth1 samples were used to examine the effects of the filler on the crystallinity of the matrix. The addition of PSMA-modified particles significantly decreased the crystallinity and melting temperature and increased the apparent size of the lamellae (Table II). The reduction in the melting temperature was possibly due to a greater amount of β-phase polypropylene present, but more tests would be needed to confirm.[32] Although a reduction in the crystallinity and an increase in the lamellar size could have been partially responsible for the increases in DBS,[33] it is unlikely that it could have been the most important effect, as similar morphological alterations were observed in the PSMA1 and Anth1 composites, whereas Anth1 significantly outperformed PSMA1 under AC voltage. These results indicate that long brush chains of PSMA were mostly responsible for changes in the matrix morphology. However, the addition of anthracene to the filler surface had little additional effect. Thus, the morphological changes, although interesting, were unlikely to be the dominant factor in the DBS improvements.

All of the composites displayed a generally aligned dispersion state because of the shear from the extrusion and pressing process used to create the test films. The cause of alignment was supported by annealed samples, where the elongated agglomerates relaxed to a spherical shape during annealing. Despite the PSMA2 system having graft density and molecular weight values in the brush similar to the PSMA1 system, the morphologies were starkly different; this indicated that exclusion of the solvent-processing step permitted the formation of large agglomerates. This may have been the ramification of brush entanglement leading to resilient interparticle bridges.[34] The dispersion states observed in the systems filled with silica grafted with PSMA and anthracene were qualitatively well explained by Daoud-Cotton theory[35] and the scaling laws presented for surface-grafted bottle-brush polymer brushes by Zhulina and Wernersson.[36,37] The calculations of brush height based on chain length and graft density place the

**Table II.** Percentage Crystallinity, Onset of the Melting Temperature, and Lamellar Size for Polypropylene and Selected Composites

| Sample | Crystallinity (%) | Melting temperature (°C) | Lamellar size (nm) |
|---|---|---|---|
| Neat polypropylene | 48 | 169 | 12 |
| As-received silica | 48 | 160 | 13 |
| PSMA1 | 35 | 149 | 15 |
| Anth1 | 34 | 152 | 17 |

three composites Anth1, 2, and 3 of the TEM micrographs in the semidilute brush, concentrated brush, and a combination of the two regimes.

According to the intuition built from the thermodynamics developed in the literature,[10] the dispersion state proceeded logically from the brush structure. The semidilute brush was capable of entangling with the matrix and with neighboring brushes but was insufficient to shield interparticle enthalpic attraction; this led to agglomerates that elongated during molding. A short, concentrated brush shielded enthalpic attractions but led to the entropy-driven dewetting of the matrix from the brush; this yielded a behavior similar to an unmodified particle. The combination of a high graft density with long chains led to a concentrated brush near the particle core capable of shielding interparticle attraction; this was also long enough to transition to the semidilute regime capable of matrix entanglement. This reduced dewetting and led to the best dispersion state seen in this study. The morphology of brushes in poor solvents and mismatched polymer melts has been shown to depend on the kinetic pathway taken to arrive at that state and may result in kinetically trapped metastable states.[38] If the brushes of two particles are entangled in a metastable state, the amount of energy needed during melt processing to separate them may be prohibitively high. This intuition was supported by the drastic differences in morphologies that arose in the PSMA1 and PSMA2 systems, despite their quite similar polymer brushes. These difference could thus only be due to the use of the solvent premix for the PSMA1 composite; by separating particles with neat polypropylene before drying, this premix should have reduced the formation of strong interparticle entanglements. These results reveal that even systems that are predicted to produce thermodynamically stable dispersed filler states can result in metastable agglomerations when inappropriate processing is used.

**Breakdown**

Figure 4 displays the AC and DC DBS data for the composites with and without anthracene surface modification. In each case, the gross morphology of the nanoparticle dispersion had a major effect on the performance of the composite; this was as significant as a change in the surface chemistry of the filler itself. The disparity between the ac and dc performance in the composite containing high-aspect-ratio agglomerates revealed that the surface treatment was responsible for substantially altering not only the DBS behavior in the nanoparticle-filled polypropylene composites but also the dispersion state, and thus, the arrangement of the particles and the trap states they induced were critical. Anthracene was demonstrated to reduce DBS under DC conditions when it was introduced as a free molecule to polypropylene. This was in line with previous work in epoxy under AC conditions, and reinforced the importance of grafting the molecule to nanoparticles if its benefits are to be realized.[16] Weibull scale parameters and their percentage change compared to the neat polypropylene are tabulated in Table III. Unsurprisingly, the systems with larger, cluster-type agglomerates performed poorly under both the AC and DC test conditions, and the addition of anthracene, although it did moderate this effect, still led to a composite with reduced performance. As shown in the literature, the improvement of the dispersion could be used to alleviate the DBS penalties that arose from filler agglomeration, and the addition of anthracene surface modification to the dispersed nanoparticle-containing composite showed a significant improvement in DBS under both conditions. The importance of the dispersion morphology on the composite's bulk properties was observed in systems with elongated agglomerates. The effects of dispersion increased in magnitude in the similarly dispersed systems with anthracene surface modification, where a disparity was observed between the AC and DC DBS performance. A possible explanation for this phenomenon was in the buildup of space charge. Nanoparticles have been demonstrated to alter the movement of space charges. In the case of an applied DC stress, the delay of a homocharge near the electrode from which it was injected lowers the local field at the interface and reduces the total injected charge.[39,40]

Large elongated agglomerates perpendicular to the field should be effective at trapping a mobile charge before it can advance into the bulk; thus, composites with such agglomerates should be expected to outperform even well-dispersed systems under dc stress. The opposite, observed under AC conditions, was hypothesized to be due to the same phenomenon. Order of magnitude calculations, with the assumption of a charge mobility in polyolefins of $5 \times 10^{-15}$ $m^2/Vs$, indicated that in one half-cycle of ac voltage near the characteristic breakdown field of 200 kV/mm, the injected charge should have moved roughly 10 nm.[41] The front of this charge may have moved significantly farther, and mobility varied. Values above $10^{-13}$ $m^2/Vs$ were measured experimentally.[42] Elongated agglomerates may have trapped some of this charge in states introduced by the nanoparticles and anthracene molecules on their surface, especially where the agglomerates were located near the surface of the composite film. When the sign of the applied voltage switched on the half-cycle, a homocharge injected from the electrode became a heterocharge[43] and should have been located nearer the electrode in systems with elongated agglomerates compared to other systems. Field enhancement due to the heterocharge proximity may have led to enhanced charge injection each half-cycle; this possibly led to a self-reinforcing runaway effect under AC test conditions. This hypothesis was supported by the data presented in Figure 7, where the percentage change in the 63% breakdown parameter is presented for dc breakdown, and two ramp rates are presented for AC breakdown. A successive increase in the injected charge was expected to build with

**Table III.** Weibull Scale Parameters for the DBS and Respective Percentage Changes for Each Composite under AC and DC Test Conditions

| Sample | AC 63% (kV/mm) | ΔAC (%) | DC 63% (kV/mm) | ΔDC (%) |
|---|---|---|---|---|
| Neat polypropylene | 200 | NA | 526 | NA |
| As received | 175 | −12 | 346 | −34 |
| PSMA1 | 196 | −2 | 445 | −15 |
| PSMA2 | 172 | −14 | 672 | 28 |
| Anth2 | 149 | −26 | 702 | 33 |
| Anth3 | 191 | −4 | 503 | −15 |
| Anth1 | 231 | 16 | 623 | 18 |

progressive ac cycles; thus, a slower ramp rate and more AC cycles should have intensified the effect. If this hypothesis was true, in addition to expecting all of the materials to display slightly lowered absolute values for DBS under slower ramp rates, we expected the composite with elongated agglomerates to display a larger decrease in the breakdown strength when normalized to the neat polypropylene control. Additionally, a dispersed system that did not suffer from the cyclic space charge reinforcing phenomenon should have retained parity to the neat polypropylene control. Both of these predictions were consistent with these data.

### Permittivity

The peak seen around $10^3$ Hz in the imaginary permittivity spectra from composites containing PSMA brushes was attributed to the relaxation of PSMA, which exhibited a relaxation in this same frequency range. Because the planes of the agglomerates were well aligned perpendicular to the field, the larger permittivity enhancement in the agglomerated systems was only marginal, unlike what was seen in systems with randomly oriented high-aspect-ratio fillers. Additionally, although poorly dispersed silica particles increased low-frequency losses, the same morphologies with anthracene showed a reduction in the imaginary permittivity below 1 Hz compared to the systems without anthracene. This was attributed to the traps introduced by anthracene surface modification; it reduced the mobility of charges otherwise contributing to low-frequency losses. The increased permittivity of composites with elongated agglomerates compared to that of similarly modified but more dispersed systems was likely due to enhanced conductivity at the filler–matrix interface; this led to field enhancement around the fillers. The elongated agglomerates with a higher aspect ratio led to a greater field enhancement than that of dispersed fillers, as shown in FEA models.[44] Anthracene on the filler surface was suspected to raise surface conduction and additionally increased this effect.

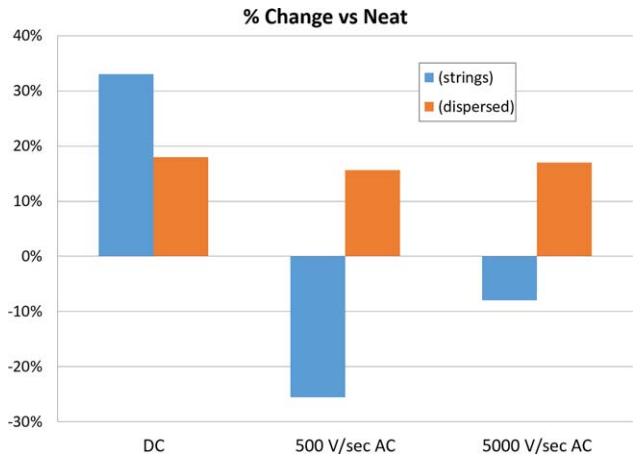


**Figure 7.** Percentage change in DBS in comparison with neat polypropylene for the neat and dispersed anthracene-modified silica NF systems under DC and two AC ramp rates. [Color figure can be viewed at wileyonlinelibrary.com]

### Voltage Endurance

The literature has shown that inorganic NFs have the potential to improve the voltage endurance of polymer-based insulation.[45–47] Because of the significant time required to gather data, only the best dispersed and elongated agglomerate composites with anthracene modification were chosen as test cases. Figure 6 shows that endurance lifetime under ac conditions was greatly improved with well-dispersed, anthracene-modified silica/polypropylene composites, whereas agglomerates with anthracene significantly reduced the time to failure. Only one stress was used for the elongated agglomerates because of the short times to failure at higher fields. Each point shows the Weibull 63% average calculated for that applied voltage, with the associated tick marks representing the bounds of a 95% confidence interval. For each voltage, a Mann-Whitney test, a nonparametric test of the null hypothesis, which may be applied to unknown distributions, indicated that the composite containing dispersed silica particles with anthracene significantly outperformed the neat polypropylene. These improvements may have been due to two combined effects. As anthracene-modified silica particles have been shown to increase the breakdown strength under ramped tests and the improvement was indicated to result from the trapping of injected charge carriers, these extrinsic traps may have been responsible for the slowing of the homocharge movement near the needle in the region of highest field concentration. Homocharge buildup lowered the local field and decreased further charge injection; this delayed the inception of an electrical tree. Additionally, silica NFs have been shown to delay erosion under partial discharge, even at low loadings.[47] Preferential erosion of the polymer results in the residual NF forming a surface coating resistant to discharge. This same phenomenon may also slow tree growth under conditions of internal partial discharges.

## CONCLUSIONS

The grafting of anthracene to silica nanoparticles and the successful polymerization of PSMA from the particle surface allowed for significant improvements to DBS. Different brushes generated dispersion states that were dependent on the brush graft density, molecular weight, and processing conditions. The dispersions included a high-aspect-ratio agglomerated system and a relatively well-dispersed system. These dispersion states were shown to occur independently of the presence or the absence of anthracene molecules on the nanoparticle surface and were as affected by the processing parameters as by the inherent thermodynamics of the brush. This indicated a need for more research in systems where the filler may be kinetically trapped in metastable states because the solvent processing used to achieve thermodynamically stable dispersions is impractical for industrial applications. Nanoparticles and the addition of anthracene to their surface increased the real permittivity by as much as 20%. The addition of anthracene also decreased the low-frequency losses compared to each anthracene-free silica-filled control with similar dispersion states; this was attributed to a decrease in the hopping conduction partially responsible for the low-frequency behavior. Dispersed silica nanoparticles with anthracene on their surfaces increased the DBS under both ac and dc test conditions by more than 15%; this was attributed to the trap states introduced by these particles interfering with electron avalanches. This same composite also displayed improved ac voltage endurance over that of the neat control. Systems with high-aspect-ratio agglomerates displayed different behaviors under ac and dc conditions; this improved the dc performance more than the dispersed particles but substantially reduced the ac breakdown performance. The hypothesis put forth in this contribution was that this effect may have been due to space charge transport being substantially altered in the system where stretched agglomerates oriented perpendicular to the applied field acted as barriers to charge motion. By trapping homocharge near the electrode, we could improve injection and ultimately breakdown strength under dc test conditions. Conversely, the same trapped charge could have caused field enhancement every half-cycle of applied ac voltage; this led to more charge injection. Calculations from the literature values of the charge mobility in polypropylene indicated that the charge may have moved on the order of 100 nm each half-cycle. This number corresponded to the length scale of the interagglomerate separation observed in the high-aspect-ratio agglomerate composite and lent some credence to this theory. These results reveal that ideal dispersion may be the best way to guarantee performance under a wide range of conditions in an isotropic material, but anisotropic, partially agglomerated dispersion states are a way to further optimize performance under specific conditions if the proper nanostructuring can be designed for the stress condition.

## REFERENCES


1. Davidson, C.; Trainer, D. Innovative Concepts for Hybrid Multi-Level Converters for HVDC Power Transmission. In 9th IET International Conference on AC and DC Power Transmission; IEEE: London, **2010**; p 1.
2. Lewis, T. J. *IEEE Trans. Dielectr. Electr. Insul.* **1994**, *1*, 812.
3. Travelpiece, A. M.; Nelson, J. K.; Schadler, L. S.; Schweickart, D. In Conference on Electrical Insulation and Dielectric Phenomena; IEEE, **2009**; p 535.
4. Zhao, S. Mechanical and Thermal Properties of Nanoparticle Filled Epoxy Nanocomposites; Rensselaer Polytechnic Institute: Troy, NY, **2007**.
5. Nelson, J. K.; Fothergill, J. C. *J. Nanotechnology* **2004**, *15*, 586.
6. Roy, M.; Nelson, J. K.; MacCrone, R. K.; Schadler, L. S.; Reed, C. W.; Keefe, R.; Zenger, W. *IEEE Trans. Dielectr. Electr. Insul.* **2005**, *12*, 629.
7. Calebrese, C.; Hui, L.; Schadler, L. S.; Nelson, J. K. *IEEE Trans. Dielectr. Electr. Insul.* **2011**, *18*, 938.
8. Rytöluoto, I.; Lahti, K.; Karttunen, M.; Koponen, M.; Virtanen, S.; Pettersson, M. *IEEE Trans. Dielectr. Electr. Insul.* **2015**, *224*, 2196.
9. Siddabattuni, S.; Schuman, T. P.; Dogan, F. *ACS Appl. Mater. Interfaces* **2013**, *5*, 1917.
10. Natarajan, B.; Li, Y.; Deng, H.; Brinson, L. C.; Schadler, L. S. *Macromolecules* **2013**, *46*, 2833.
11. Tao, P.; Li, Y.; Siegel, R. W.; Schadler, L. S. *J. Mater. Chem. C* **2013**, *1*, 86.
12. Tao, P.; Viswanath, A.; Li, Y.; Siegel, R.; Benicewicz, B. C.; Schadler, L. S. *Polymer* **2013**, *54*, 1639.
13. Meli, L.; Arceo, A.; Green, P. F. *Soft Matter* **2009**, *5*, 533.
14. Natarajan, B.; Neely, T.; Rungta, A.; Benicewicz, B. C.; Schadler, L. S. *Macromolecules* **2013**, *46*, 4909.
15. Akcora, P.; Liu, H.; Kumar, S. K.; Moll, J.; Li, Y.; Benicewicz, B. C.; Schadler, L. S.; Acehan, D.; Panagiotopoulos, A. Z.; Pryamitsyn, V. *Nat. Mater.* **2009**, *8*, 354.
16. Krentz, T. M.; Huang, Y.; Nelson, J. K.; Schadler, L. S.; Bell, M.; Benicewicz, B. In 2014 Annual Report Conference on Electrical Insulation and Dielectric Phenomena; IEEE: Des Moines, IA, **2014**; p 643.
17. Li, Y.; Tao, P.; Viswanath, A.; Benicewicz, B. C.; Schadler, L. S. *Langmuir* **2013**, *29*, 1211.
18. Yamano, Y. *IEEE Trans. Dielectr. Electr. Insul.* **2006**, *13*, 773.
19. Sparks, M.; Mills, D.; Warren, R.; Holstein, T.; Maradudin, A. A.; Sham, L. J.; Loh, E. J.; King, D. F. *Phys. Rev. B* **1981**, *24*, 3519.
20. O'Dwyer, J. J. *J. Phys. Chem. Solids* **1967**, *28*, 1137.
21. Bamji, S. S.; Bulinski, A.; Abou-Dakka, M.; Mclntyre, D. In Annual Report Conference on Electrical Insulation and Dielectric Phenomena; IEEE: **2009**; p 662.
22. Abou-Dakka, M.; Ghunem, R. A.; McIntyre, D. In Conference on Electrical Insulation and Dielectric Phenomena (CEIDP); IEEE: **2014**; p 723.
23. Roy, M.; Nelson, J. In Conference on Electrical Insulation and Dielectric Phenomena; IEEE: **2005**; p 1.
24. Yamano, Y.; Ilzuka, M. In Proceedings of 2008 International Symposium on Electrical Insulating Materials; IEEE: **2008**; p 392.

25. Das-Gupta, D. K.; Barbarez, M. K. *J. Phys. D* **1973**, *6*, 867.
26. Seitz, F. *Phys. Rev.* **1949**, *76*, 1376.
27. Qiao, Y.; Yin, X.; Wang, L.; Islam, M. S.; Benicewicz, B. C.; Ploehn, H. J.; Tang, C. *Macromolecules* **2015**, *48*, 8998.
28. Song, Y. S.; Youn, J. R. *Carbon* **2005**, *43*, 1378.
29. Bond, E.; Spruiell, J.; Lin, J. *J. Polym. Sci. Part B: Polym. Phys.* **1999**, *37*, 3050.
30. Smith, R.; Liang, C.; Landry, M.; Nelson, J.; Schadler, L. *IEEE Trans. Dielectr. Electr. Insul.* **2008**, *15*, 187.
31. Holto, J.; Ildstad, E. In Proceedings of the 2010 IEEE International Conference on Solid Dielectrics; IEEE: **2010**; p 1.
32. Jacoby, P. Beta Nucleating Masterbatch Offers Enhanced Properties in Polypropylene Products; **2007**.
33. Ieda, M. *Electr. Insul. IEEE Trans.* **1980**, *15*, 206.
34. Loverso, F.; Egorov, S. A.; Binder, K. *Macromolecules* **2012**, *45*, 8892.
35. Daoud, M.; Cotton, J. P. *J. Phys.* **1982**, *43*, 531.
36. Zhulina, E. B.; Vilgis, T. A. *Macromolecules* **1995**, *28*, 1008.
37. Wernersson, E.; Linse, P. *Langmuir* **2013**, *29*, 10455.
38. Williams, D. R. M. *J. Phys. II* **1993**, *3*, 1313.
39. Castellon, J.; Agnel, S. In Annual Report Conference on Electrical Insulation and Dielectric Phenomena; IEEE: **2006**; p 345.
40. Ma, D.; Hugener, T. A.; Siegel, R. W.; Christerson, A.; Mårtensson, E.; Önneby, C.; Schadler, L. S. *Nanotechnology* **2005**, *16*, 724.
41. Sahli, S.; Bellel, A.; Ziari, Z.; Kahlouche, A.; Segui, Y. *J. Electrostat.* **2003**, *57*, 169.
42. Baum, E. A.; Lewis, T. J.; Toomer, R. *J. Phys. D* **1978**, *11*, 703.
43. Bamji, S.; Abou-Dakka, M.; Bulinski, A. *IEEE Trans. Dielectr. Electr. Insul.* **2007**, *14*, 77.
44. Wang, Z.; Keith Nelson, J.; Hillborg, H.; Zhao, S.; Schadler, L. S. *Compos. Sci. Technol.* **2013**, *76*, 29.
45. Takala, M.; Ranta, H.; Nevalainen, P.; Pakonen, P.; Pelto, J.; Karttunen, M.; Virtanen, S.; Koivu, V.; Pettersson, M.; Sonerud, B. IEEE Trans. Dielectr. Electr. Insul. **2010**, *17*, 1259.
46. Roy, M.; Nelson, J. K.; MacCrone, R. K.; Schadler, L. S. *J. Mater. Sci.* **2007**, *42*, 3789.
47. Iizuka, T.; Zhou, Y.; Maekawa, T.; Tanaka, T.; Tatsumi, K. *Conf. Electr. Insul. Dielectr. Phenom.* **2014**, *5*, 703.